Title

ADSORPTION AND SURFACE REACTIONS OF H[SUB]2 S AND SO[SUB]2 ON CU(100) STUDIED BY ELECTRON ENERGY LOSS SPECTROSCOPY

Authors

Leung, K.T.
Zhang, X.S.
Shirley, D.A.

Publication Date

1988-12-01

LBL-25552
Preprint

Lawrence Berkeley Laboratory
UNIVERSITY OF CALIFORNIA

Materials & Chemical Sciences Division

Submitted to Journal of Physical Chemistry

Adsorption and Surface Reactions of H_2S and SO_2 on Cu(100) Studied by Electron Energy Loss Spectroscopy

K.T. Leung, X.S. Zhang, and D.A. Shirley

December 1988

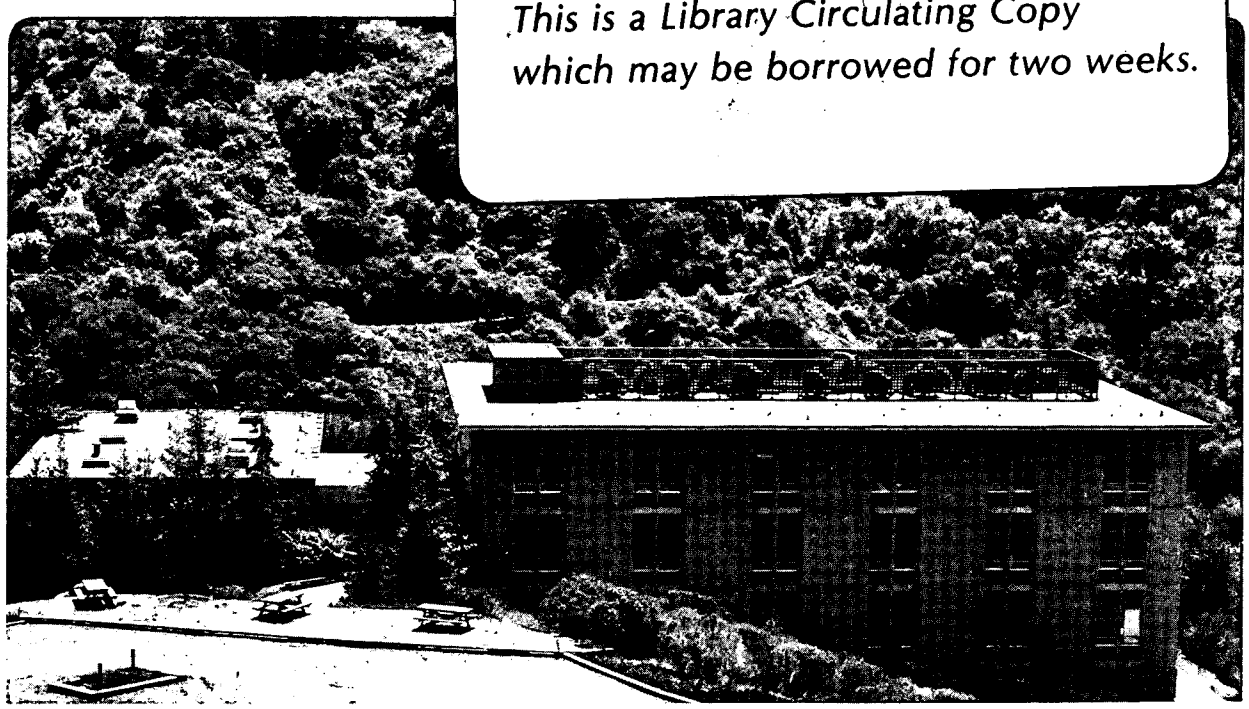

Prepared for the U.S. Department of Energy under Contract Number DE-AC03-76SF00098.

DISCLAIMER

Adsorption and Surface Reactions of H_2S and SO_2 on Cu(100) Studied by Electron Energy Loss Spectroscopy

K.T. Leung,* X.S. Zhang# and D.A. Shirley

Department of Chemistry
University of California
and
Materials and Chemical Sciences Division
Lawrence Berkeley Laboratory
1 Cyclotron Road
Berkeley, California 94720
U.S.A.

ABSTRACT

The adsorption of H_2S and SO_2 on Cu(100) were investigated using electron energy loss spectroscopy as a function of coverage, temperature and scattering angles. In particular, irreversible dissociation of H_2S and the formation of sulfhydryl (SH) species at low and intermediate coverage on Cu(100) were observed at low temperature. This was followed by molecular physiadsorption at higher coverage. In the case of SO_2 on Cu(100), decomposition of SO_2 and the formation of SO_3 surface species at room temperature were observed. A surface reaction involving pre-adsorbed SO_2 on Cu(100) with H_2S is discussed.

*Present address: Department of Chemistry, University of Waterloo, Waterloo, Ontario N2L 3G1, Canada.

#Permanent address: Department of Physics, Zhejiang University, Hongzhou, People's Republic of China.

I. INTRODUCTION

Since the pioneering work of Propst and Piper,[1] electron energy loss spectroscopy (EELS)[2] has become a popular, non-destructive technique for surface analysis when high surface sensitivity is desired. Detailed information concerning the bonding of various surface adsorbates and their intermediates can be obtained from their characteristic vibrational spectra.[3-8] Many surface intermediates[9-11], as well as their adsorption and desorption behaviour, have been identified by EELS. Furthermore, recent developments in electron optics have allowed the study of the kinetics of surface reactions involving these surface species.[12]

The adsorption behaviours of H_2S and SO_2 on surfaces have attracted a great deal of attention because of the industrial and environmental importance of these molecules. Adsorption properties of H_2S on Rh(100),[13] Mo(100),[14] MoS_2,[15] Si(111)[16] and GaAs[17] have been investigated by a variety of techniques including low energy electron diffraction (LEED), photoemission, thermal desorption and EELS. Of particular interest are the photoemission studies of H_2S on Ru(110),[18] W(100),[19] and GaAs surfaces,[17] and the electron energy loss studies of H_2S on Ni(100)[20] and Pt(111),[21] which reported the formation of sulfhydryl (SH) species, at low temperature in most cases.[18,20,21] Two different interpretations of the corresponding vibrational features were also presented in the latter two EELS studies.[20,21]

Similarly, a number of studies involving different techniques were reported for the adsorption of SO_2 and its reactions on metal surfaces. Blyholder and Cagle showed that the reaction of SO_2 on Fe and Ni produced SO_4 surface species.[22] A similar reaction involving SO_4 as a product on Ag was also reported by Barber *et al.* using secondary ion mass spectroscopy[23] and by Lassiter using Auger electron spectroscopy and work function measurements.[24] Low, Goodsel and Takezawa, on the other hand, studied the adsorption of SO_2 on CaO[25] and on MgO[26] at room temperature using Fourier transform infrared spectroscopy and suggested SO_3 as a possible surface species upon adsorption. Kohler and Wassmuth[28] investigated the kinetics of SO_2 on Pt(111) using a molecular beam technique and thermal desorption measurements, and further suggested that SO_2 adsorbed dissociatively at low temperature for small coverages. Dissociative adsorption involving a

wide range of possible surface species was also observed on other surfaces, including Rh(110),[29] Pt(110),[29] Pt(111)[28] and Pd(100)[30] near liquid nitrogen temperatures. However, a recent study by Hussla and Heidberg[27], using far and mid infrared transmission spectroscopy, found no evidence of dissociative adsorption for SO_2 on Cu(100) over a wide temperature range. On Ag(100), Ag(111), Ag(110),[31] and Au,[32] molecular adsorption at low temperature and dissociative adsorption at higher temperature[31] were reported.

An earlier publication[20] from this laboratory gave a detailed characterization of the adsorption and decomposition of H_2S on Ni(100). In this report, we present a parallel study on the adsorption of H_2S and SO_2 on Cu(100) using EELS. Surface species generated from the adsorption and desorption of H_2S and SO_2 on Cu(100), as well as from reactions between H_2S and a Cu(100) surface pre-adsorbed with SO_2, were characterized using the measured electron energy loss spectra. Except for the differences in the values of the vibrational frequencies, very similar adsorption and decomposition behaviours can be inferred from the vibrational spectra associated with these surface species on Cu(100) and Ni(100)[20] in the case of H_2S. For SO_2, similar adsorption patterns were found on Cu(100) and Ag(110).[31]

II. EXPERIMENTAL

The angle-resolved electron energy loss spectrometer was housed in an UHV chamber (base pressure = $1x10^{-10}$ torr), which was equipped with retarding-field optics capable of LEED and Auger electron spectroscopy (AES) as well as an ion sputtering gun for sample cleaning. A detailed description of our modified electron energy loss spectrometer was given elsewhere.[33] Briefly, it consisted of a 2-inch mean diameter double-pass hemispherical monochromator and a 5-inch mean diameter single-pass hemispherical analyzer. The analyzer was rotatable in both polar and azimuthal directions with respect to the normal of the crystal to facilitate off-specular measurements without rotating the sample. Two separate three-aperture lenses were used as the output optics for the monochromator and as the input optics for the analyzer. In the earlier design, the double hemispheres of the monochromator were separated by a single aperture. In the present work, the aperture was replaced by a three-aperture lens to enable the two hemispheres to operate at different

pass energies.[34] This modification improved the signal rate by a factor of 5-10 while maintaining similar energy (40 cm^{-1} FWHM) and angular (3° half-angle) resolution.

A high purity Cu crystal was cut, polished and oriented to within 1° from the (100) plane by standard methods. It was (pre-)cleaned by a well-known procedure: repeated cycles of Ar ion sputtering at 1 keV followed by annealing at 800 K for 15 minutes. The cleanliness of the sample was checked using retarding-field AES. The sample could be cooled to liquid nitrogen temperature or heated to above 1500 K using electron beam bombardment from the back of the sample plate. The temperature of the crystal was measured using a chromel-alumel thermocouple spot-welded on the sample plate 7 mm above the crystal. The accuracy of the temperature measurements was estimated to be $\pm$ 20 K.

Detailed descriptions of the effusive beam dosing procedure as well as the calibration procedure using an ambient dosing technique were given elsewhere.[20,33] Exposures of H_2S (Matheson, 99.5% purity) or SO_2 (Matheson, 99.98% purity) was achieved by maintaining an ambient chamber pressure of $1x10^{-9}$ torr with the adsorbant for a specified period of time with the sample positioned at 1 cm from an effusive beam doser. Exposures obtained by this beam dosing technique were calibrated with those obtained using an ambient dosing procedure, by comparing the corresponding S(152 eV) to Cu(62 eV) relative Auger intensities. A $1x10^{-8}$ torr-sec exposure using the beam dosing procedure corresponded to 0.5-1 L (1 L = $1x10^{-6}$ torr-sec). A saturation coverage was obtained after 40 L and 20 L exposures of H_2S and SO_2, respectively. A new sample was prepared for each exposure, to avoid accumulative contamination.

All specular EELS measurements were made at an incident angle of 55° from the surface normal, while off-specular measurements were conducted by rotating the analyser through a fixed angle from the specular direction, away from the surface normal. An impact energy of 1.6 eV was used for all measurements. Individual peaks in the EEL spectra were deconvoluted using a combination of gaussians as well as a background function to approximate the tail of the elastic peak. The accuracy of the reported loss frequencies so determined was estimated to be $\pm$ 4 cm^{-1}.

III. RESULTS

A. EELS of H_2S/Cu(100)

Figure 1 shows the EEL spectra of a Cu(100) surface exposed to a saturation coverage of H_2S and recorded at (a) 100 K and (b) 300 K in the specular direction. A diffuse p(2x2) LEED pattern with streaks between the quarter and half order spots was observed at both temperatures, with the pattern obtained at 100 K being more diffuse. Further annealing of the sample at 300 K to ca. 500 K for 10 minutes produced a sharp p(2x2) LEED pattern with no observable streaks. Good agreement is observed between the reported p(2x2)S/Cu(100) spectrum[8] and the room temperature spectrum (Fig. 1b). In particular, the dissociation of H_2S on Cu(100) is indicated by the strong S-Cu stretch observed at 324 cm^{-1}. The small downward shift (ca. 12 cm^{-1}) relative to the reported S-Cu stretch[8] can be attributed to possible disorder effects for the dissociated species on Cu(100) at room temperature. There is also some evidence of phonon vibrations,[7] as indicated by the weak shoulder at 177 cm^{-1}. The spectrum at 100 K (Fig. 1a) shows four additional peaks at 430, 550, 1144 and 2469 cm^{-1}. The two higher vibrational features at 1144 and 2469 cm^{-1} can be readily identified respectively as H-S bending and stretching modes of molecularly adsorbed H_2S by a comparison with the available vibrational data of free H_2S molecules.[35] In the gas-phase data the 1290 and 2611 (2684) cm^{-1} peaks were assigned to H-S bending and symmetric (asymmetric) stretching modes, respectively. The feature at 178 cm^{-1} in the 100 K spectrum can be attributed to either surface phonon vibration as in the room temperature case or hindered translations of molecularly adsorbed H_2S.

In order to identify the remaining features (i.e. at 430 and 550 cm^{-1}), an EEL spectrum of a saturation coverage of D_2S on Cu(100) at 100 K was measured (Fig. 2b). The effect of isotopic substitution is to scale the frequencies of the H-related vibrations of H_2S/Cu(100) with respect to those of the corresponding vibrations of D_2S/Cu(100) by a factor of $\sqrt{2}$. The frequencies of these two systems as well as the gas-phase data are given in Table 1. The observed D_2S/Cu(100) features are consistent with the isotopic substitutional effect, with the scaling factors lying between 1.2 and 1.4. The D-S stretching modes of the molecularly adsorbed D_2S were not observed, presumably due

to their weak intensities. The broad structure at 317 cm^{-1} may be due to an overlap of two features: the scaled analog of the H_2S feature at 430 cm^{-1} and the S-Cu stretch. The features at 430 (317) and 550 (452) cm^{-1} for H_2S (D_2S) are therefore related to surface vibrations involving H (D) atoms.

Figure 3 shows the EEL spectra of a saturation coverage of H_2S on Cu(100) at 100 K measured in the specular and two off-specular scattering geometries. Assuming that the S-Cu stretch (at 320 cm^{-1}) is dipole active, one can obtain a qualitative idea of the dipole (infrared) activity of other structures by comparing the changes in their intensities relative to the S-Cu stretch as a function of angle. This comparison confirms that the H-S bend (at 1144 cm^{-1}) and H-S stretch (at 2469 cm^{-1}) of molecularly adsorbed H_2S have non-dipole (i.e. impact-scattering) contributions, as indicated by a large increase in the relative intensities in the 10° off-specular spectrum (note scale change in Fig. 3c). In other words, H_2S is adsorbed on the Cu surface such that these vibrations have parallel components in the dipole moments with respect to the surface. Furthermore, the feature at 430 cm^{-1}, like the S-Cu stretch (at 320 cm^{-1}), is dipole active. Together with the evidence obtained in Fig. 2, we may identify this structure to be H-S stretch of a sulfhydryl (SH) species with S bonded in a head-on configuration perpendicular to the surface. Finally, the angular variation of the remaining feature at 550 cm^{-1} is similar to that of the H-S stretch of the dissociated (SH) species. This may likely be due to a second H-S vibrational mode or a H-Cu vibration. Further evidence is required to distinguish between the two possibilities.

A temperature dependent study is shown in Figure 4. In this experiment, the Cu(100) surface was first exposed with a saturation coverage of H_2S at 100 K (Fig. 4a). It was subsequently annealed to the specified temperatures for 5 minutes. The sample was then recooled back to 100 K, at which temperature the EEL spectrum was recorded. It should be noted that a new sample was prepared for each run to avoid accumulative contamination. Fig. 4b shows that the anneal at 130 K removed the two molecular features at high frequency as well as the structure at 430 cm^{-1}. The removal of the two high frequency features suggests that H_2S was physisorbed on Cu(100) below 130 K. Furthermore, the dissociated SH species, which gave rise to the feature at 430 cm^{-1}, was weakly adsorbed. The marked increase in the intensities of the S-Cu stretch and of the vibration at

550 cm^{-1} (Fig. 4b) further suggests that the SH species may (1) dissociate to form S (abs.) and H (abs.), and/or (2) rearrange itself to a different site or a different vibrational mode. Finally, further annealing to higher temperatures resulted in a gradual decrease in the intensities of the remaining features at 320 and 550 cm^{-1}. A significant depletion in the intensity of the 178 cm^{-1} peak after the 130 K anneal was also observed, suggesting that the 178 cm^{-1} peak may have a contribution from the hindered translations of molecularly adsorbed H_2S. Its residual intensity after the 130 K anneal (Figs. 4c to 4e) can be attributed to phonon vibration. Qualitatively, we may conclude that the adsorption strength of the observed features increases in the following order: {178, 430, 1144, 2469 cm^{-1}} (weak) < 550 cm^{-1} < 320 cm^{-1} (strong).

Finally, we present a coverage dependent study (using a beam dosing procedure)[20,33] to investigate the early stages of H_2S adsorption on Cu(100) in Figure 5. The most striking change is the red shift of the feature at 600 cm^{-1} at low coverage (Fig. 5a) to 550 cm^{-1} at saturation coverage (Fig. 5e). There is no other noticeable change in the frequencies of the other features with coverage. At low coverages (Figs. 5a and 5b), H_2S appears to dissociate into S and a species (most likely H) which gives rise to the feature at 550 cm^{-1} at saturation coverage. These dissociated species saturate at an exposure of about 20 seconds (1-2 L) before the SH species (at 430 cm^{-1}) and the molecularly adsorbed H_2S begin to accumulate. This is consistent with the order of adsorption strength of individual species asserted in the temperature dependent study (Fig. 4) above. Furthermore, it confirms that H_2S dissociates to S (and H) at low coverage on Cu(100) at 100 K.

B. EELS of SO_2/Cu(100)

Figure 6 shows the EEL spectra of a saturation coverage of SO_2 on Cu(100) exposed and measured in the specularly reflected direction at two different temperatures. Table 2 summarizes plausible assignments of the observed frequencies, compared with those of free SO_2 molecules and other SO_2 related systems. Except for the low frequency region (<500 cm^{-1}), two markedly different vibrational spectra were observed. By comparing with the gas-phase data,[35] the peaks at 1290, 978 and 515 cm^{-1} in the 100 K spectrum (Fig. 6a) can be assigned to antisymmetric stretch, symmetric stretch and bending modes respectively. The two S-O stretching frequencies are lower

than the corresponding gas-phase data (c.f. 1362 cm^{-1} for symmetric stretch and 1151 cm^{-1} for asymmetric stretch) while the bending frequency at 515 cm^{-1} is almost identical to the corresponding gas-phase data.[35] The remaining broad band is treated as an envelope of two close lying peaks at 346 and 290 cm^{-1}. The feature at 346 cm^{-1} corresponds closely to the S-Cu stretching frequency of S/Cu(100)[8] (c.f. 336 cm^{-1}) while the peak at 290 cm^{-1} may be interpreted as either a torsion mode or hindered translations of physiadsorbed SO_2. The low frequency part of the room temperature spectrum (Fig. 6b) can be assigned in an analogous fashion as the 100 K spectrum. Three different peaks are observed at 859, 613 and 482 cm^{-1}. We postpone discussion of the assignments of these vibrations until later. It should also be noted that the width of the elastic peak changes significantly, from 44 cm^{-1} FWHM at 300 K to 60 cm^{-1} FWHM at 100 K. The peak broadening effect is an indication of surface disorder arising from physiadsorption. This interpretation is supported by an increase in the diffuseness in the observed p(2x2) LEED pattern of the sample at 100 K compared to that at 300 K.

Figure 7 shows the vibrational spectra of SO_2 on Cu(100) at 300 K as a function of coverage obtained using a beam dosing procedure.[20,33] The coverages of the 10s, 20s and 30s spectra correspond approximately to 1/3, 2/3 and 1 monolayer, respectively. There is very little change in the spectrum except for the structure at 859 cm^{-1}, which increases proportionally with coverage.

A saturation coverage of SO_2 on Cu(100) at 300 K was annealed to 350 K and 500 K for 5 minutes using electron beam bombardment from the back of the sample. Drastic changes were observed in the vibrational spectra, shown in Figure 8. The low temperature anneal to 350 K completely removed the high frequency features at 613 and 859 cm^{-1} and sharpened the low frequency band at 324 cm^{-1}. Further annealing to 500 K did not produce any noticeable change. There is also some evidence of a weak shoulder near 172 cm^{-1} after the anneal. By comparing the annealed spectra with that of S/Cu(100),[8] it is clear that the 172 cm^{-1} feature corresponds to a phonon vibration while the feature at 324 cm^{-1} is due to S-Cu stretch (Figs. 8b and 8c).

Finally, a saturation coverage of SO_2 on Cu(100) at 300 K was exposed to 12 L of H_2S using an ambient dosing procedure. The EEL spectrum shown in Figure 9 indicates a very similar

vibrational profile to the spectra of the annealed sample shown in Fig. 8. In particular, the high frequency features are not observed and the feature at 329 cm^{-1} can again be attributed to S-Cu stretch.[8] Like the annealed spectra (Fig. 8), the weak shoulder at 161 cm^{-1} provides some evidence of a possible phonon vibration.

IV. DISCUSSION

A. Adsorption of H_2S on Cu(100)

For C_{2v} triatomic molecules adsorbed on surfaces, up to 9 vibrational modes may become infrared active. These include 3 normal modes and 6 additional modes including 3 hindered rotations and 3 hindered translations. The assignments of the observed surface vibrations of H_2S on Cu(100) are consistent with both the gas-phase data[35] and the earlier EELS data of S/Cu(100).[8] In particular, the S-Cu stretch (at 320 cm^{-1}) is identified by comparison with the reported S/Cu(100) EELS study[8] (Fig. 1a). The assignments of the features at 1144 and 2469 cm^{-1} to molecular H-S bending and stretching modes respectively are unambiguous. The vibration at 178 cm^{-1} can be attributed to either phonon vibrations or hindered translations of molecularly adsorbed H_2S. The latter case is supported by a coordinated increase (Fig. 5) and decrease (Fig. 4) in the intensity of this structure concomitant with the other molecularly adsorbed H_2S features at 1144 and 2469 cm^{-1}.

The features at 430 and 550 cm^{-1} are more difficult to interpret. Very similar EELS spectra of H_2S on Ni(100)[20] and on Pt(111)[21] were also reported. Both studies assigned the lower frequency peak to H-S stretch[20] or H-S bend[21] but gave two different assignments to the higher frequency, H-related feature analogous to the one observed at 550 cm^{-1} in the present work. In particular, Baca *et al.*[20] assigned the higher frequency vibration to H-Ni stretch while Koestner *et al.*[21] identified the corresponding peak to a second H-S bend. These two studies also reported similar temperature-dependent adsorption behaviours of H_2S as in the present work, with the higher (lower) frequency vibrations of the respective systems becoming stronger (weaker) at higher temperature. In the case of H_2S/Pt(111), however, an earlier study by Baro *et al.*[36] identified a fairly strong low frequency mode due to H-Pt asymmetric stretch with H adsorbed in a hollow site. This feature persisted in the spectra if the sample was annealed to 220 K, in direct analog with the strong

adsorption of the higher frequency feature observed by Koestner *et al.*[21] The assignment of Baca *et al.* (i.e. to H-metal stretch) therefore appears to be more consistent with the data of both Pt(111) studies[36,21] and the present case. The assignments of the features at 550 cm^{-1} and 430 cm^{-1} to a H-Cu stretch with H in a stable (probably four-fold hollow) site and to H-S vibrations (bend or stretch) of a sulfhydryl species, respectively, are in accord with the observed changes in the relative intensities of the angle-dependent spectra (Fig. 3). The existence of atomic H on Cu(100) is also consistent with an earlier study which suggested that the adsorption of H_2 on Cu(100) involved atomic chemisorption and that activated dissociation was involved.[3] The reported EELS study of H_2 on Cu(100)[3] indicated that H_2 adsorbed molecularly only below 10 K. It should be noted that we cannot, however, rule out an alternative assignment of the feature at 430 cm^{-1} to hindered rotations of molecularly adsorbed H_2S. Nevertheless, judging from the small intensity of this peak and the absence of the feature at 178 cm^{-1} at low coverage (Figs. 5a and b), which we earlier suggested to be due to hindered translations, this assignment appears to be rather unlikely.

Both Fisher[18] and Baca *et al.*[20] proposed a similar model for the adsorption of H_2S on Ru(110) and Ni(100), respectively, at liquid nitrogen temperature. In this model, complete irreversible dissociation of H_2S into S (ads.) and H (ads.) at low coverage is followed by partial dissociation into H-S (ads.) and H (ads.) at intermediate coverage. The H (ads.) may recombine to form H_2 which is then desorbed from the surface. Finally, molecular adsorption of H_2S is observed at high coverage, most likely in the form of islands. This model appears to be consistent with the present EELS data of H_2S on Cu(100) at 100 K, as evidenced by the coverage-dependent study (Fig. 5). Without a detailed calculation of the vibrational spectrum assuming different surface structures, it is difficult to determine the bonding sites or geometries of the observed surface species: S, H, SH and H_2S from the EELS spectra. The initial dissociation of H_2S into S and H at low coverage probably leaves the dissociated species in the most stable (four-fold hollow) site which leads to perpendicular surface vibrations. The similarity between the S-Cu stretching frequency in the present case and that of the S/Cu(100) case[8] confirms this model. The small value of the H-Cu stretching frequency also suggests that H is adsorbed in a four-fold site although as pointed out by

Baca *et al.*[20] one cannot unambiguously identify the site based only upon the magnitude of the vibrational frequency. At intermediate and higher coverage, it is not clear from the frequencies of the weakly bonded SH and H_2S species what bonding sites that these species may occupy. In fact the nature of the H-S vibration (i.e. whether it is a stretching or bending mode) is not clear. However, the intensity variation of this feature as a function of scattering angle (Fig. 3) indicates a strong dipole contribution. For the SH species it is therefore more likely, though not conclusively, that the H-S stretching mode is being observed. For the molecular H_2S species, there are similar difficulties in identifying the adsorption sites, although the associated frequencies allow us to distinguish between the stretching and bending modes.

Unlike H_2O,[5,6] for which molecular adsorption on metal surfaces appears to be the rule, the dissociation of H_2S and the formation of sulfhydryl (SH) species appear to be quite common on most metal surfaces studied to date. Except for W(100)[19] where it occurred at room temperature, SH formation occurred below 170 K on most metal surfaces, including Rh(100),[13] Ru(110),[18] Ni(100),[20] Pt(111),[21] and Cu(100). Like molecularly adsorbed H_2S, the SH species binds weakly to the surface and desorbs easily. This behaviour can be attributed to the much smaller H-S bond energy in H_2S when compared with the H-O bond energy in H_2O. The desorption behaviour of H_2S on Cu(100) is also very similar to that observed on the other metal surfaces,[13,18,20,21] where H_2 and H_2S appear to be the only desorption products. In particular, thermal desorption studies of H_2S on Pt(111)[21] and on Rh(100)[13] suggested two molecular H_2S desorption states: one due to chemisorbed H_2S interacting with the sulfided metal surfaces and the other due to H_2S weakly bonded within islands of chemisorbed H_2S. This picture of weak H_2S adsorption is consistent with the temperature dependent EELS study in the present work.

B. Adsorption of SO_2 on Cu(100)

In the case of SO_2 adsorption, the three high frequency features at 100 K (Fig. 6a) can be assigned to the corresponding normal modes of free SO_2 molecules by a comparison with the gas-phase data.[35] (See Table 2). The low frequency features at 346 and 290 cm^{-1} are most likely due to S-Cu stretch and hindered translations, respectively. The similarity of the observed vibrational

features with those of free SO_2 molecules[35] and S/Cu(100)[8] suggests that SO_2 was physisorbed on the surface at 100 K. A similar adsorption pattern was also reported for SO_2 on CsCl films.[27] In particular, associative adsorption on CsCl was observed for three different adsorption phases involving different temperature ranges: α phase (220-240 K), β phase (146-205 K), and γ phase (>200 K). The characteristic frequencies corresponding to these phases are given in Table 2. In the case of SO_2 on CsCl,[27] only one low-frequency peak, presumably due to S-CsCl stretch, was reported although there were significant backgrounds in these infrared spectra. The assignment of the feature at 290 cm^{-1} in the SO_2 on Cu(100) case to hindered translation is therefore not unique. Other possibilities include: (1) a torsion mode, and (2) two different adsorption sites for SO_2 molecules which give rise to two possible S-Cu vibrational frequencies. The EEL spectrum of 12 L of SO_2 on Pd(100) recorded at 115 K by Burke and Madix[30] was very similar. In both cases, the frequencies of the observed (molecular) features compare favourably with the corresponding ones for solid SO_2.[38]

The spectral features of the room temperature spectrum (Fig. 6b) are more difficult to interpret. The low frequency features (290 and 340 cm^{-1}) at 300 K could be assigned in a similar fashion as for the low temperature spectrum. No high-frequency peaks (>1000 cm^{-1}), characteristic of the SO_2 internal vibrations that were observed in the low temperature case, were found. The three new features observed at 482, 613 and 859 cm^{-1} were indicative of different surface species (other than SO_2) resulting from the room temperature adsorption. Previous studies of SO_2 on Fe and Ni,[22] Ag films,[23,24] Pt(111),[28] Pd(100)[30] and p(2x2)S/Pd(100)[30] all suggested dissociative adsorption and reported evidence of SO_4 and S as the principal adsorption products, particularly at higher temperatures. Other studies of SO_2 on CaO[25] and MgO,[26] however, suggested SO_3 as a possible surface species upon adsorption. The EELS study of the oxidation of SO_2 on Ag(110) reported by Outka *et al.*[31] suggested the presence of SO_3 and SO_4 at different temperatures. From Table 2, the strong peaks at 859 and 613 cm^{-1} and the weak feature at 482 cm^{-1} can be tentatively assigned respectively to symmetric/asymmetric S-O stretch, symmetric S-O bend and asymmetric S-O bend of SO_3. The band at 859 cm^{-1} is broad and can be attributed to two overlapping bands. Earlier

infrared data relating the SO_x (x = 3 or 4) vibrations suggested that in general the asymmetric S-O stretching frequency is greater than 1100 cm^{-1} for SO_4 but smaller than 1100 cm^{-1} for SO_3.[31] The relatively low value of the S-O stretching band at 859 cm^{-1} therefore strongly favours the presence of SO_3 rather than SO_4.

The sulfite group, SO_3, can coordinate to the metal surface as an unidentate or bidentate ligand. Both of these bonding arrangements were considered for the case of SO_3 on Ag(110) by Outka *et al.*,[31] who concluded from their EEL spectra that unidentate O-bonding occurred between 200-325 K while bidentate bonding was found between 325-500 K. From the infrared data of the coordination complexes compiled by Outka *et al.*,[31] O-coordination with SO_3 in a pyramidal arrangement (see Table 2) appears to be most likely for Cu(100). This is consistent with Nyberg and Larsson's observation that a strong vibration above 975 cm^{-1} is indicative of S-coordination.[40] In the case of bidentate geometry, there are at least four possible cases, each involving bonding of a S-O pair or an O-O pair to either one or two metal atoms. From the infrared studies of bidendate coordination complexes of the type $[Co(en)_2SO_3]X$ where X= ClO_4^-, NO_2^-, I^- or SCN^-, it was found that the spectrum would be more complex due to the existence of many different vibrations.[37] The simplicity of our spectrum further supports that unidentate coordination through the O atom represents the most probable bonding geometry.

From the observed vibrational spectrum at 300 K, we have already concluded that the reaction: $SO_2 + SO_2 \rightarrow$ S (abs.) + SO_4 (abs.) involving the production of SO_4 is unlikely. Instead, surface reactions generating SO_3 and S (and/or O) as adsorbed surface species are considered. We therefore propose the following reaction scheme to account for the observed adsorption pattern.

(1) $SO_2 \rightarrow$ SO (abs.) + O (abs.)

(2) SO (abs.) + $SO_2 \rightarrow$ S (abs.) + SO_3 (abs.)

(3) O (abs.) + $SO_2 \rightarrow$ SO_3 (abs.)

(4) SO (abs.) $\rightarrow$ S (abs.) + O (abs.) at higher coverage or above 350 K

This model (reactions 1-3) is certainly not unique in accounting for the observed S (abs.) and SO_3 (abs.) species. It emphasizes dissociative adsorption of SO_2 into SO (abs.) and O (abs.)

(reaction 1), which subsequently combines with SO_2 to give SO_3 (abs.) (reaction 3). The reaction of SO (abs.) with SO_2 gives the products S (abs.) and SO_3 (abs.) (reaction 2). As evident from the coverage-dependent spectra (Fig. 7), the increase in the intensity of the S-O stretching modes but not the bending modes at higher coverages suggests the build-up of additional species other than SO_3. In this model, the most likely candidate is SO itself. Furthermore, additional dissociation of SO into S and O (reaction (4) above) cannot be ruled out. It should be noted that both S-Cu[8] and O-Cu[9] stretching modes occur at the same frequency and it is therefore impossible to differentiate between the two. The two low frequency features at 296 and 340 cm^{-1} can also be explained by the presence of two different S-Cu (stretching) vibrations corresponding to Cu-SO or Cu-SO_3. This implies that both SO and SO_3 are present at all coverages and SO continues to build up after the saturation of SO_3 on the surface. With the present resolution of 40 cm^{-1} FWHM, it is not possible to resolve these two features and investigate their intensity variations as a function of coverage. The surface species (SO or SO_3) appear to be weakly adsorbed because only a small temperature rise is required to remove most of the vibrational features associated with these species (Fig. 8). After annealing, the low frequency band sharpens and can again be attributed to a S-Cu (or O-Cu) stretch. As well, the possibility of dissociation of SO and SO_3 to S and/or O cannot be ruled out.

C. Reaction of H_2S with preadsorbed SO_2 on Cu(100)

Except for the increase in the intensity of the 329 cm^{-1} peak, an exposure of 12 L of H_2S to preadsorbed SO_2 on Cu(100) at room temperature produced an almost identical spectrum (Fig. 9) to that of the annealed sample (Fig. 8). We suggested above that SO_3 is the most likely surface species upon adsorption of SO_2 on Cu(100) at room temperature. The increase in S-Cu stretch in the resulting vibration spectrum (Fig. 9b) suggests the formation of S (abs.) although it is not possible to identify the reactions involved definitively without other experimental data such as thermal desorption. This spectrum also shows that any reaction involving the formation of SH (abs.) is unlikely because the characteristic vibration at 430 cm^{-1} is missing. The SH species can, however, act as an intermediate. One possible reaction scheme would involve the dissociation of H_2S to H and SH, which would then undergo further dissociation to H and S (abs.). The dissociation of the

SH species at room temperature is consistent with the earlier temperature-dependent study shown in Fig. 4. The resulting H may combine with SO_3 to form H_2SO_3. Further study is required to substantiate this proposed mechanism.

ACKNOWLEDGEMENTS

This work was supported by the Director, Office of Energy Research, Office of Basic Energy Sciences, Chemical Science Division of the U.S. Department of Energy under contract no. DE-AC03-76SF00098. One of us (K.T.L.) gratefully acknowledges support from the Natural Sciences and Engineering Research Council of Canada and the Killam Memorial Foundation.

REFERENCES

[1] F.M. Propst and T.C. Piper, J. Vac. Sci. Technol. **4**, 53 (1967).

[2] H. Ibach and D.L. Mills, "Electron Energy Loss Spectroscopy and Surface Vibrations", Academic Press, New York (1982).

[3] S. Andersson and J. Harris, Phys. Rev. Lett. **48**, 545 (1982).

[4] M. Persson, S. Andersson and P.A. Karlsson, Chem. Phys. Lett. **111**, 597 (1984).

[5] B.A. Sexton, J. Vac. Sci. Technol. **16**, 1033 (1979).

[6] S. Andersson, C. Nyberg and C.G. Tengstal, Chem. Phys. Lett. **104**, 305 (1984).

[7] S. Andersson, B.N.J. Persson, M. Persson and N.D. Lang, Phys. Rev. Lett. **52**, 2073 (1984).

[8] M. Persson and S. Andersson, Surf. Sci. **117**, 352 (1982).

[9] B.A. Sexton, Surf. Sci. **88**, 319 (1979).

[10] B.N.J. Persson and R. Ryberg, Phys. Rev. Lett. **48**, 549 (1982).

[11] B.A. Sexton, Surf. Sci. **88**, 299 (1979).

[12] S.D. Kevan and L.H. Dubois, Rev. Sci. Instrum. **55**, 1604 (1984); W. Ho, J. Vac. Sci. Technol. **A3**, 1432 (1985); and references therein.

[13] R.I. Hegde and J.M. White, J. Phys. Chem. **90**, 296 (1986).

[14] J.M. Wilson, Surf. Sci. **57**, 499 (1976); L.J. Clarke, Surf. Sci. **102**, 331 (1981).

[15] M. Salmeron, G.A. Somorjai, A. Wold, R. Chianelli and K.S. Liang, Chem. Phys. Lett. **90**, 105 (1982).

[16] K. Fujiwara and H. Ogata, Surf. Sci. **72**, 157 (1978).

[17] J. Massies, P. Etienne, F. Dezaly and N.T. Linh, Surf. Sci. **99**, 121 (1980); W. Ranke, H.J. Kuhn and J. Finster, Surf. Sci. **192**, 81 (1987), and references therein.

[18] G.B. Fisher, Surf. Sci. **87**, 215 (1979).

[19] A.K. Bhattacharya, L.J. Clarke, L.M. De La Garza, J. Chem. Soc. Faraday Trans. **177**, 2223 (1981).

[20] A.G. Baca, M.A. Schulz and D.A. Shirley, J. Chem. Phys. **81**, 6304 (1984).

[21] P.J. Koestner, M. Salmeron, E.B. Kollin and J.L. Gland, Chem. Phys. Lett. **125**, 134 (1986).

[22] G.D. Blyholder and G.W. Cagle, Environmental Sci. & Tech. **5**, 158 (1971).

[23] M. Barber, P. Sharpe and J.C. Vickerman, Chem. Phys. Lett. **27**, 436 (1974).

[24] W.S. Lassiter, J. Phys. Chem. **76**, 1289 (1972).

[25] M.J.D. Low, A.J. Goodsel and N. Takezawa, Environmental Sci. & Tech. **5**, 1191 (1971).

[26] A.J. Goodsel, M.J.D. Low and N. Takezawa, Environmental Sci. & Tech. **6**, 268 (1972).

[27] I. Hussla and J. Heidberg, J. Electron Spectrosc. Relat. Phenom. **39**, 213 (1986).

[28] U. Kohler and H.W. Wassmuth, Surf. Sci. **126**, 448 (1983); and references therein.

[29] R.C. Ku and P. Wynblatt, Appl. Surf. Sci. **8**, 250 (1981).

[30] M.L. Burke and R.J. Madix, Surf. Sci. **194**, 223 (1988).

[31] D.A. Outka, R.J. Madix, G.B. Fisher and C. D. Maggio, J. Phys. Chem. **90**, 4051 (1986); R. Rouida and F. Pratesi, Surf. Sci. **104**, 609 (1981); and references therein.

[32] C.R. Brundle, A.F. Carley, Faraday Discuss. Chem. Soc. **60**, 51 (1975); M. Furuyama, K. Kishi and S. Ikeda, J. Electron Spectrosc. Relat. Phenom. **13**, 59 (1978).

[33] M.A. Schulz, M.Sc. Thesis, University of California, Berkeley (1985), LBL-19769; A.G. Baca, Ph.D. Thesis, University of California, Berkeley (1985), LBL-19099.

[34] L.L. Kesmodel, J. Vac. Sci. Technol. **A1**, 1456 (1983).

[35] T. Schimanouchi, "Tables of Molecular Vibrational Frequencies", Vol. 1, National Bureau of Standards, U.S. Department of Commerce, Washington, D.C. (1972).

[36] A.M. Baro, H. Ibach and H.D. Bruchmann, Surf. Sci. **88**, 384 (1979).

[37] K. Natamato and P.J. McCarthy, "Spectroscopy and Structure of Metal Chelate Compounds", Wiley, New York, p. 267 (1968).

[38] A. Anderson and S.H. Walmsley, Mol. Phys. **10**, 391 (1966).

[39] K. Nakamato, "Infrared Spectra of Inorganic and Coordination Compounds", Wiley, New York, (1963).

[40] B. Nyberg and R. Larsson, Acta. Chem. Scand. **27**, 63 (1973).

FIGURE CAPTIONS

Figure 1:

EEL spectra of a saturation coverage of H_2S on Cu(100) exposed and recorded at (a) 100 K and (b) 300 K. The FWHMs of the elastic peaks and the peak locations are indicated in cm^{-1}.

Figure 2:

EEL spectra of a saturation coverage of (a) H_2S and (b) D_2S on Cu(100) at 100 K.

Figure 3:

EEL spectra of a saturation coverage of H_2S on Cu(100) at 100 K as a function of scattering geometries: (a) specular at 55°, (b) 5° off-specular and (c) 10° off-specular (note the change in the scaling factor for (c) only). The scaling factors of individual parts of the spectra are with respect to the corresponding elastic intensities, which are not normalized to each other.

Figure 4:

EEL spectra of a saturation coverage of H_2S on Cu(100) at 100 K after different temperature treatments. The annealing temperature (in K) and time (in seconds) are indicated in each spectrum.

Figure 5:

EEL spectra of H_2S on Cu(100) at 100 K as a function of coverage. The number of seconds of exposure using an effusive beam dosing method is indicated in each spectrum. A 10 sec exposure by this procedure corresponds to 0.5-1 L (1 L = $1x10^{-6}$ torr-sec). The spectrum corresponding to a saturation coverage (~40 L) is given in (e).

Figure 6:

EEL spectra of a saturation coverage of SO_2 on Cu(100) exposed and recorded at (a) 100 K and (b) 300 K. The FWHMs of the elastic peaks and the peak locations are indicated in cm^{-1}.

Figure 7:

EEL spectra of SO_2 on Cu(100) at 300 K at different coverages. The number of seconds of exposure using an effusive beam dosing method is indicated in each spectrum. The spectrum corresponding to a saturation coverage (~20 L) is given in (d).

Figure 8:

EEL spectra of a saturation coverage of SO_2 on Cu(100) at 300 K after different temperature treatments. The annealing temperature (in K) and time (in seconds) are indicated in (b) and (c).

Figure 9:

EEL spectra of a saturation coverage of SO_2 on Cu(100) at 300 K before (a) and after (b) exposing an additional 12 L of H_2S.

TABLES

Table 1: Comparison of vibrational frequencies ($\pm$4 cm^{-1}) of adsorbed H_2S and D_2S on Cu(100) at 100 K with gas-phase data.[35]

Vibration	Gas-Phase			Adsorbed on Cu(100) at 100 K		
	(a) H_2S	(b) D_2S	Ratio (a/b)	(c) H_2S	(d) D_2S	Ratio (c/d)
H-S stretch				2469	----	----
asymmetric	2684	1999	1.34			
symmetric	2611	1892	1.38			
H-S bend	1290	934	1.38	1144	859	1.33
H-Cu stretch				550	452	1.22
H-S stretch or bend				430	317	1.36
S-Cu stretch				320	317	
Phonon or hindered translations				178		

Table 2: Comparison of vibrational frequencies (± 4 cm^{-1}) of free SO_2, SO_2 adsorbed on metal, and other oxides of sulphur.*

Systems	Frequencies (cm^{-1})							
	(a)	(b)	(c)	(d)	(e)	(f)	(g)	References
SO_2/Cu(100)								this work
at 100K	290	346	515		978		1290	
at 300K	296	340	482	613	859			
SO_3/Ag(110)								[31]
at 241K	220			585	835	885		
at 418K	245			585	805	875	1180	
SO_4/Ag(110)								[31]
at 570K	220			605	910	1070	1275	
at 815K	225			610	915		1285	
SO_2/Pd(100)								[30]
at 115K				545		1155	1355	
at 371K				525	865	1155	1250	
SO_2/CsCl								[27]
α(220-240K)	302		526			1135	1304	
β (146-205K)	215		541			1143	1297	
γ (>200K)	305		537			1119	1259	
SO_2 gas			518			1151	1362	[35]
SO_2, solid			521			1147	1308,1330	[38]
SO_3^{-2}								
pyramidal			461	633	961	1010		[39]
planar			532	652		1069	1330	
SO_4^{-2}			454	622	983	1110		[39]

*Tentative assignments: (b): metal-S stretch; (c), (d): S-O bend; (e), (f), (g): S-O stretch.

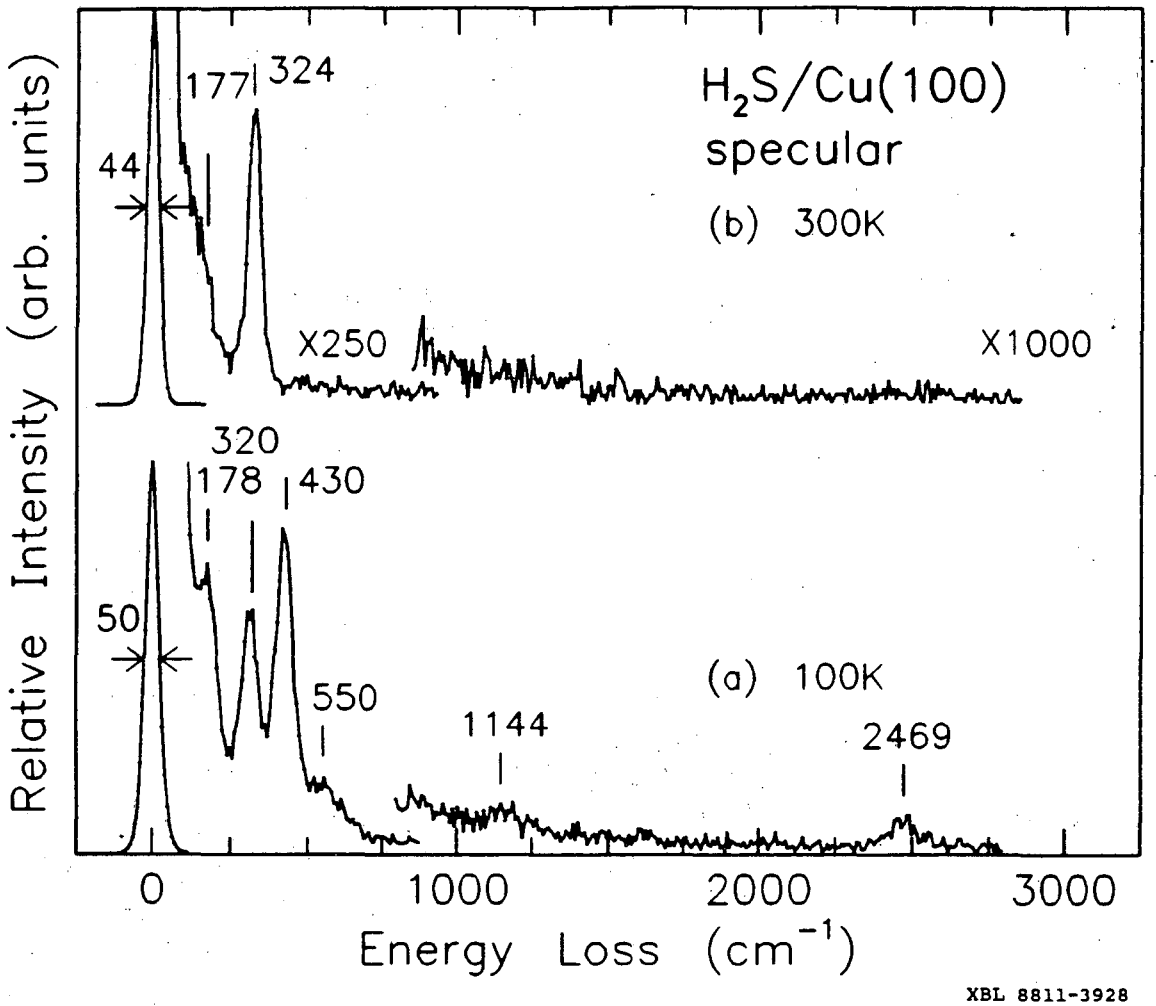

Fig. 1 Leung et al.

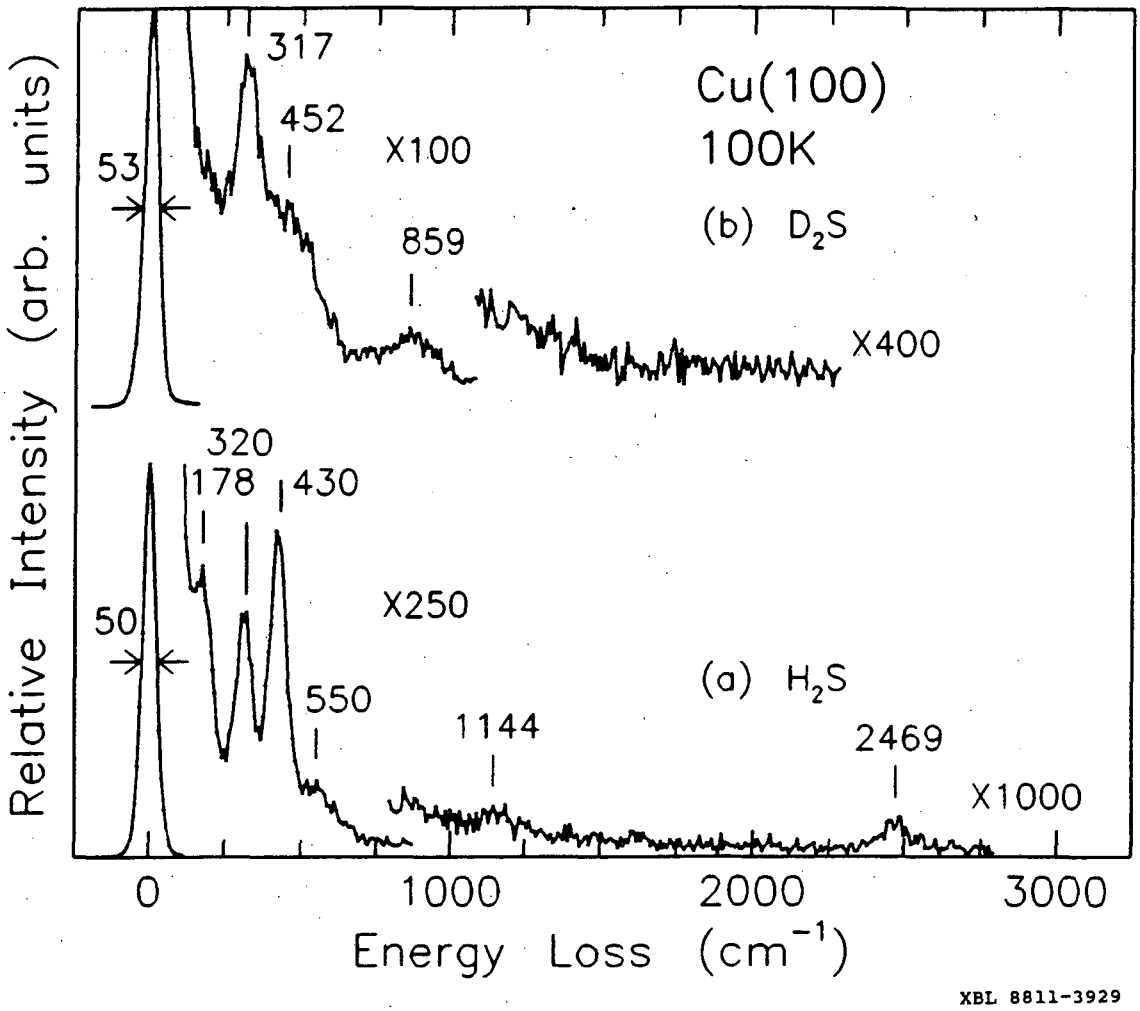

Fig. 2 Leung et al.

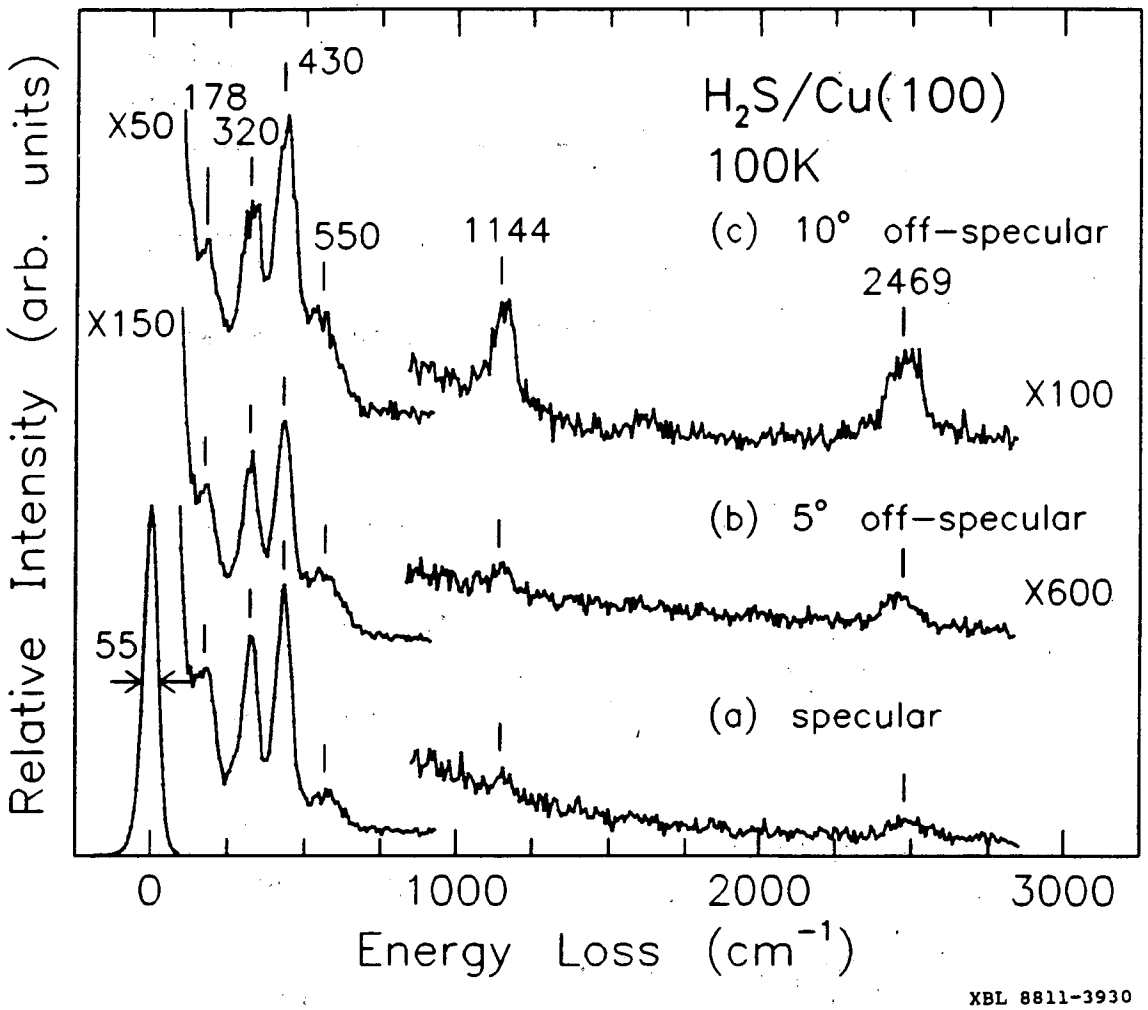

Fig. 3 Leung et al.

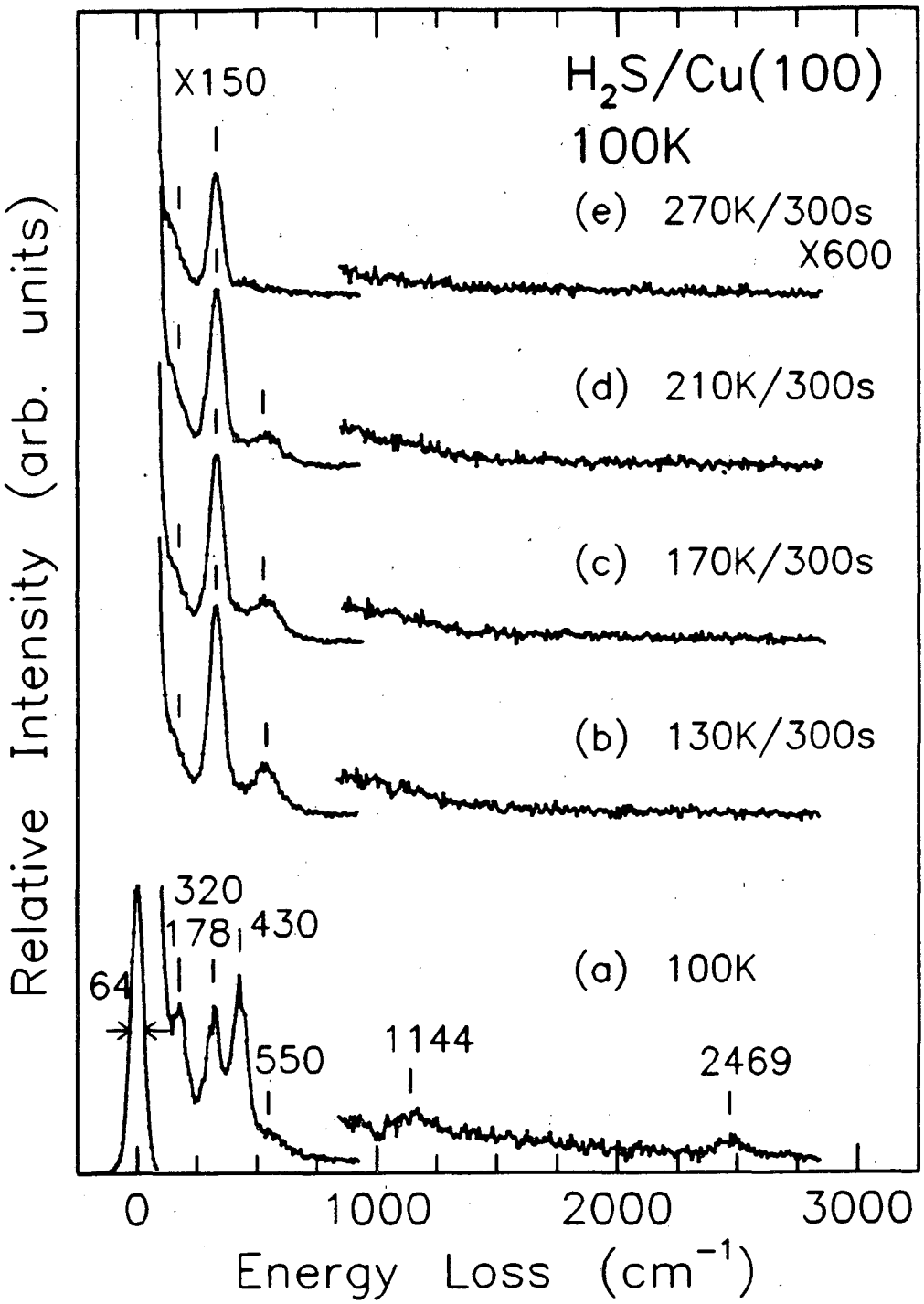

XBL 8811-3931

Fig. 4 Leung et al.

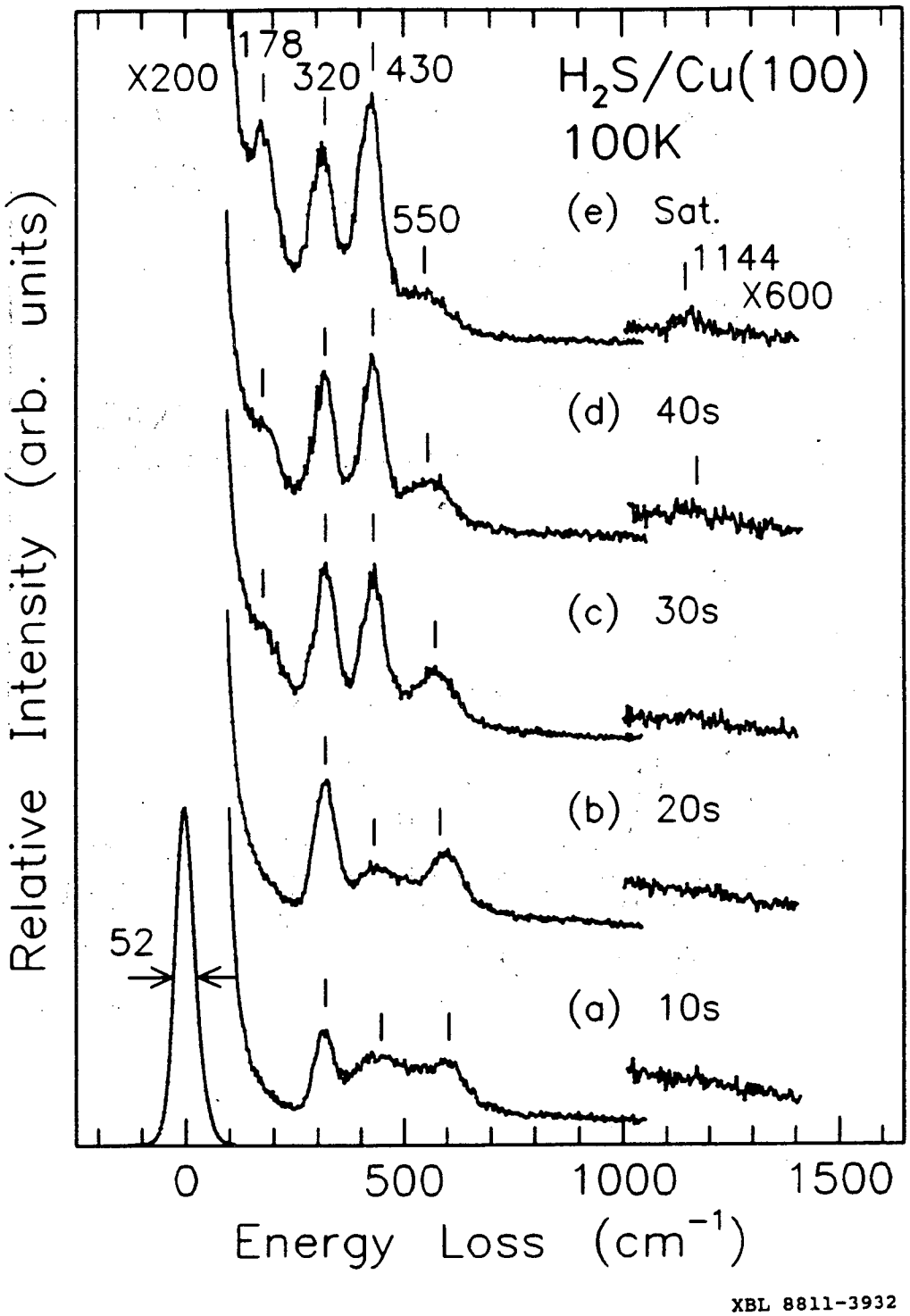

Fig. 5 Leung et al.

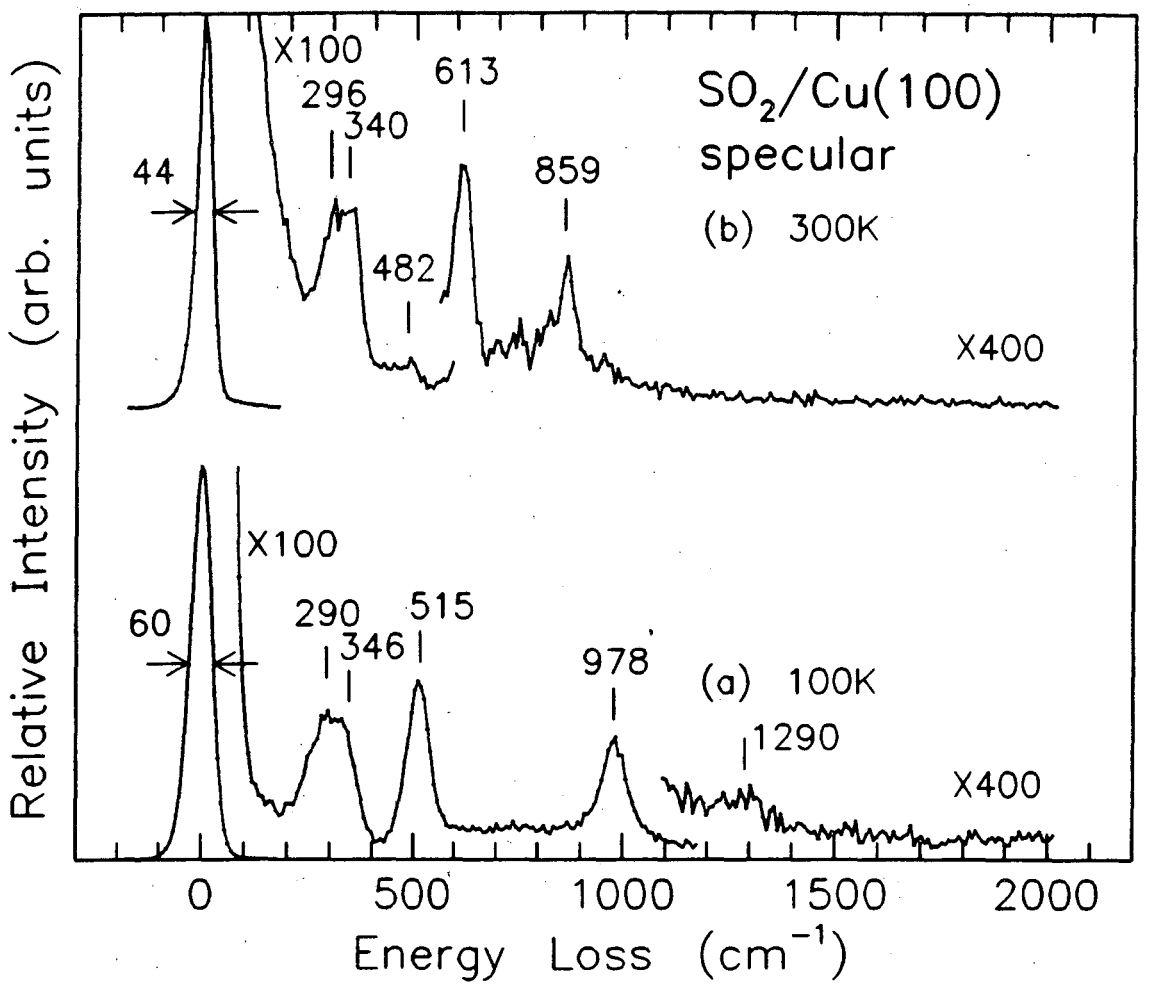

Fig. 6 Leung et al.

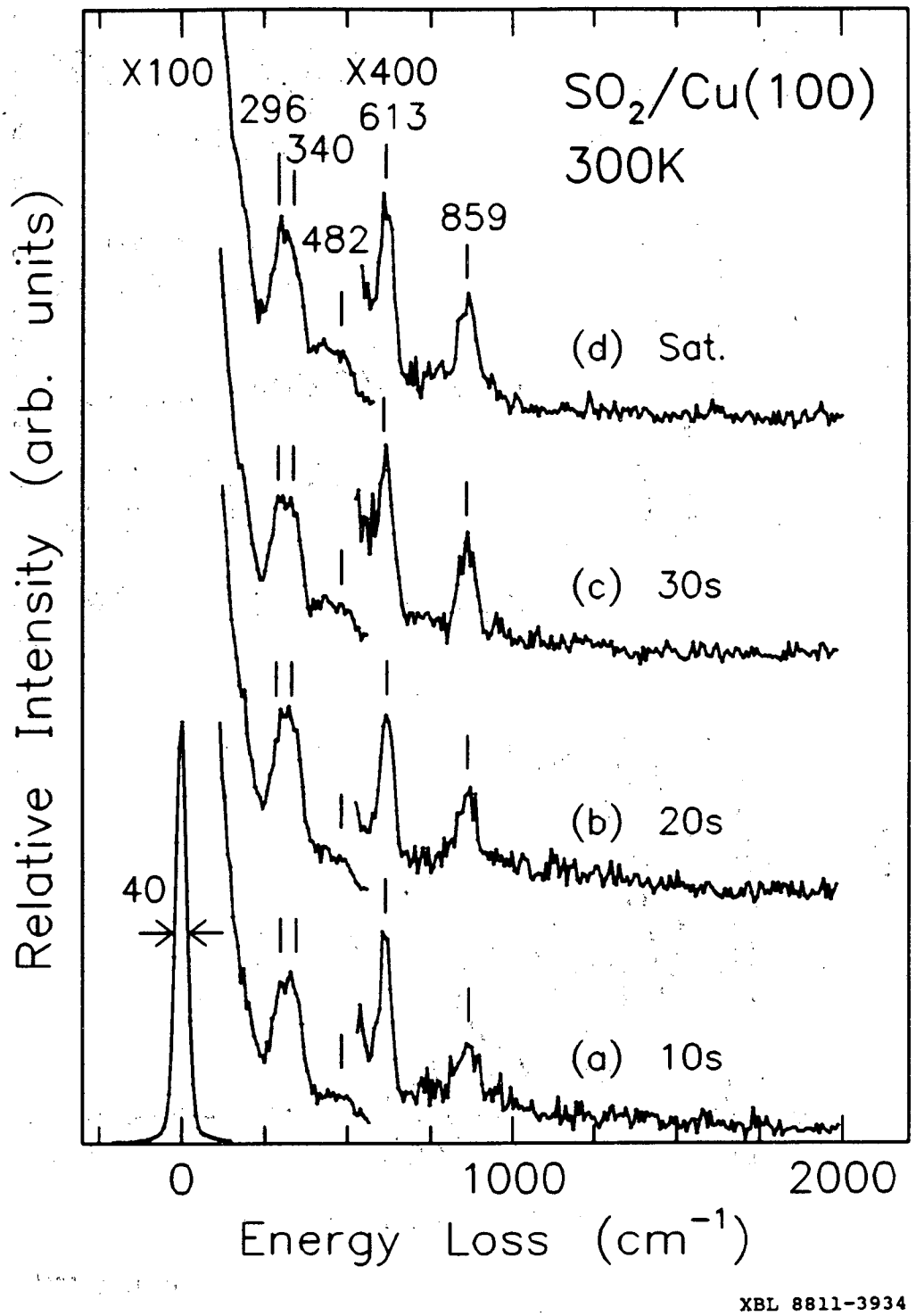

Fig. 7 Leung et al.

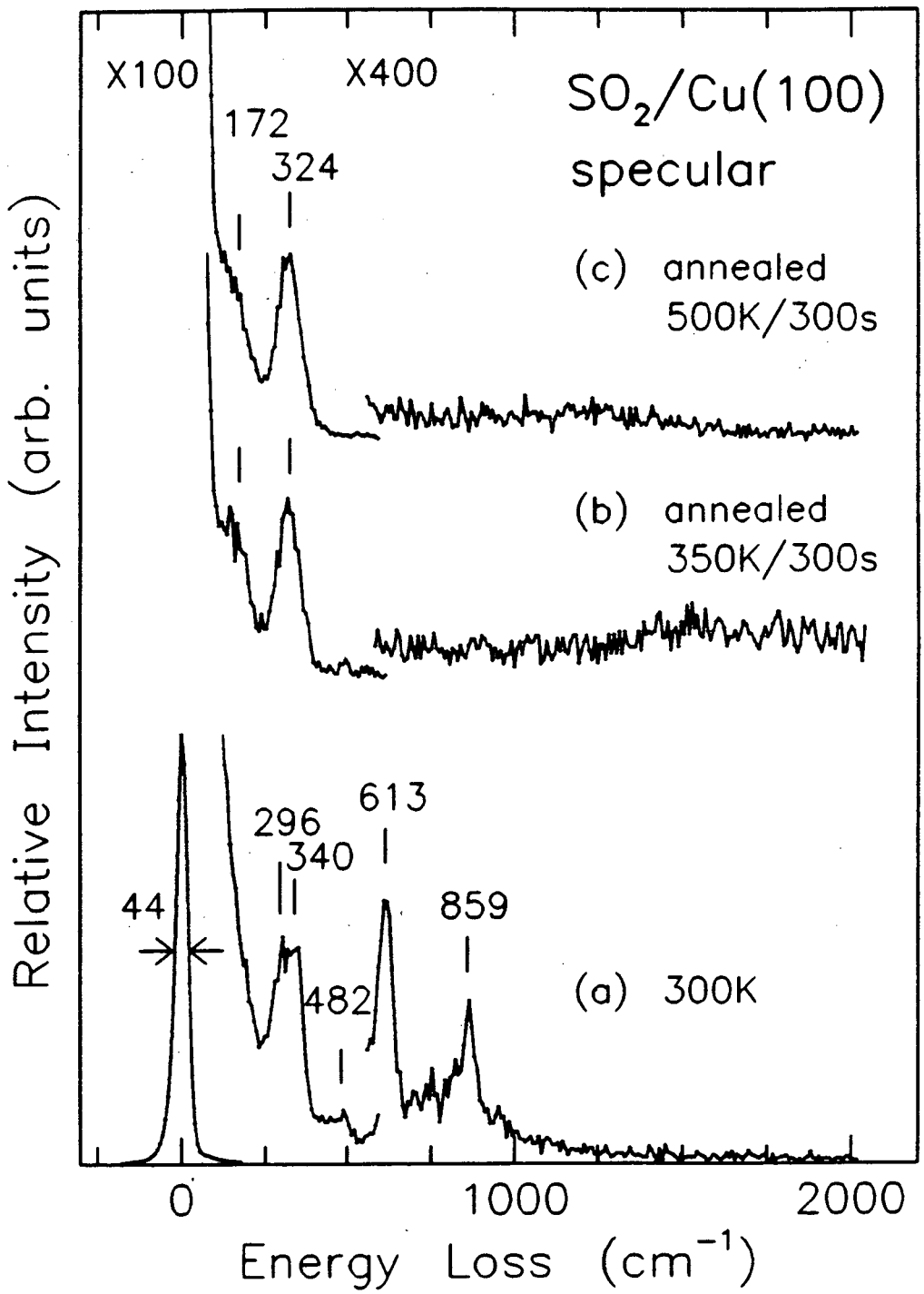

XBL 8811-3935

Fig. 8 Leung et al.

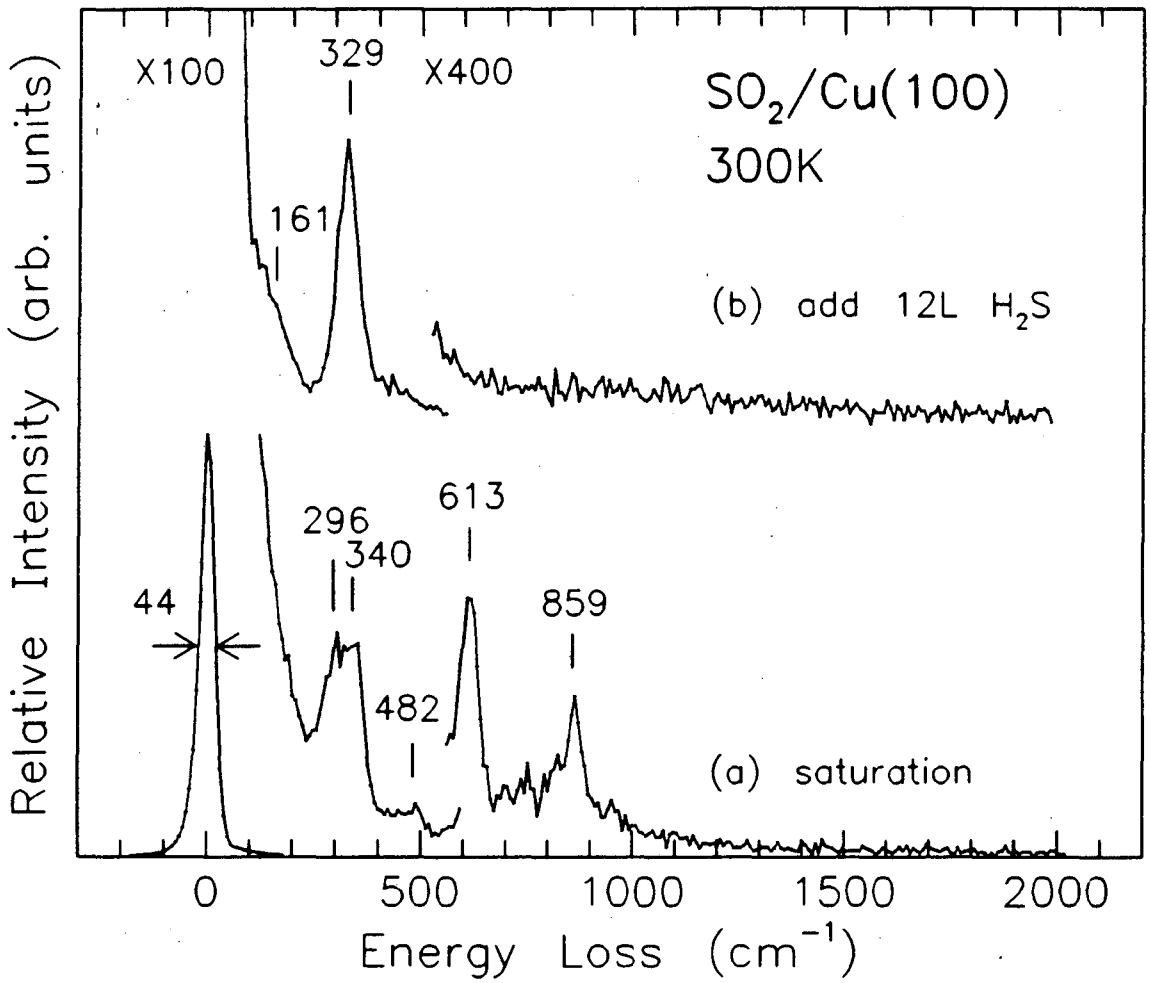

Fig. 9 Leung et al.

LAWRENCE BERKELEY LABORATORY
TECHNICAL INFORMATION DEPARTMENT
UNIVERSITY OF CALIFORNIA
BERKELEY, CALIFORNIA 94720